Supplementary Information (SI) for Journal of Materials Chemistry B.

Electronic Supplementary Information (ESI)

Simulation of bone remodelling microenvironment by the calcium compound-loaded hydrogel fibrous membranes for in situ bone regeneration

Yanmei Wu,[a#] Zhen Wu[a,b#] Zhe Li and Youliang Hong[a*]

[a] *National Engineering Research Center for Biomaterials, College of Biomedical Engineering, Sichuan University, Chengdu 610064, P. R. China*
[b] *School of Medicine and Health, Zhengzhou Research Institute, Harbin Institute of Technology, Zhengzhou, Henan 450000, China*

* Corresponding author. hyl@scu.edu.cn (Y. Hong);
# These authors contributed equally to this work.

Table S1. The primers used for qPCR analyses

Symbol		Primers
BMP-2	Forward	5’-GAAGCCAGGTGTCTCCAAGAG-3’
	Reverse	5’-GTGGATGTCCTTTACCGTCGT-3’
OCN	Forward	5’-TGACAAAGCCTTCATGTCCAA-3’
	Reverse	5’-CTCCAAGTCCATTGTTGAGGTAG-3’
OPN	Forward	5’-CCAAGCGTGGAAACACACAGCC-3’
	Reverse	5’-GGCTTTGGAACTCGCCTGACTG-3’
Runx-2	Forward	5’-CCCAACTTCCTGTGCTCCGT-3’
	Reverse	5’-AGTGAAACTCTTGCCTCGTCC-3’
GAPDH	Forward	5’- GACATGCCGCCTGGAGAAAC-3’
	Reverse	5’- AGCCCAGGATGCCCTTTAGT-3’

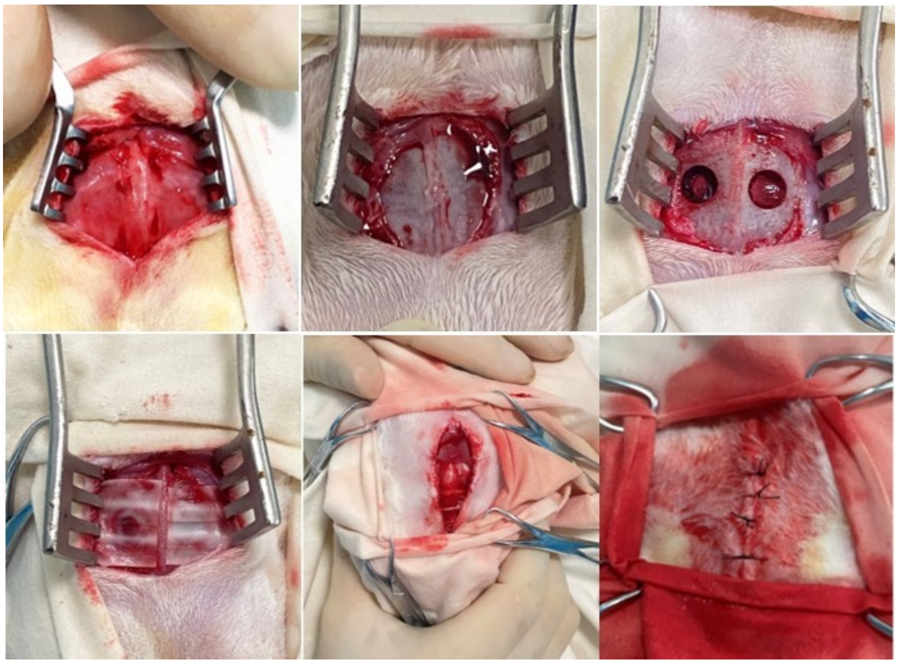

Figure S1. The surgery process of implanting the ultrathin fibrous membranes in the skull of rabbit. In detail, the midline incision, extending from the nasofrontal to occipital region (~3 cm), was cut (Top left), and the subcutaneous tissue was dissected along the same line as the skin (Top middle). The underlying periosteum was incised on the midline and subsequently two bone defects (6 mm) were created to remove bone from the left and right of the dorsal calvarium using a trephine with caution to prevent damage to the underlying sagittal sinus and dura matter (Top right). The defect edge was ground using a tip drill to get a regular circular defect. The square fibrous membranes were covered on the top of the cranial defects, and the fibre aligned orientation of the fibrous membranes was oriented perpendicular to the cranial midline (Bottom left). After the fiber membranes were implanted, the muscle and skin were sealed (Bottom middle and right).

Table S2. The mechanical properties of the as-electrospun fibrous membranes.

	Tensile modulus [MPa]	Ultimate stress [MPa]	Elongation at break [%]
SF	71.62	1.76	8.16
SF/G	26.96	0.72	6.84
SF/G-CaSL	34.55	0.79	7.74
SF/G-CaHP	49.54	0.62	6.79
SF/G-TCaP	34.97	0.68	8.41

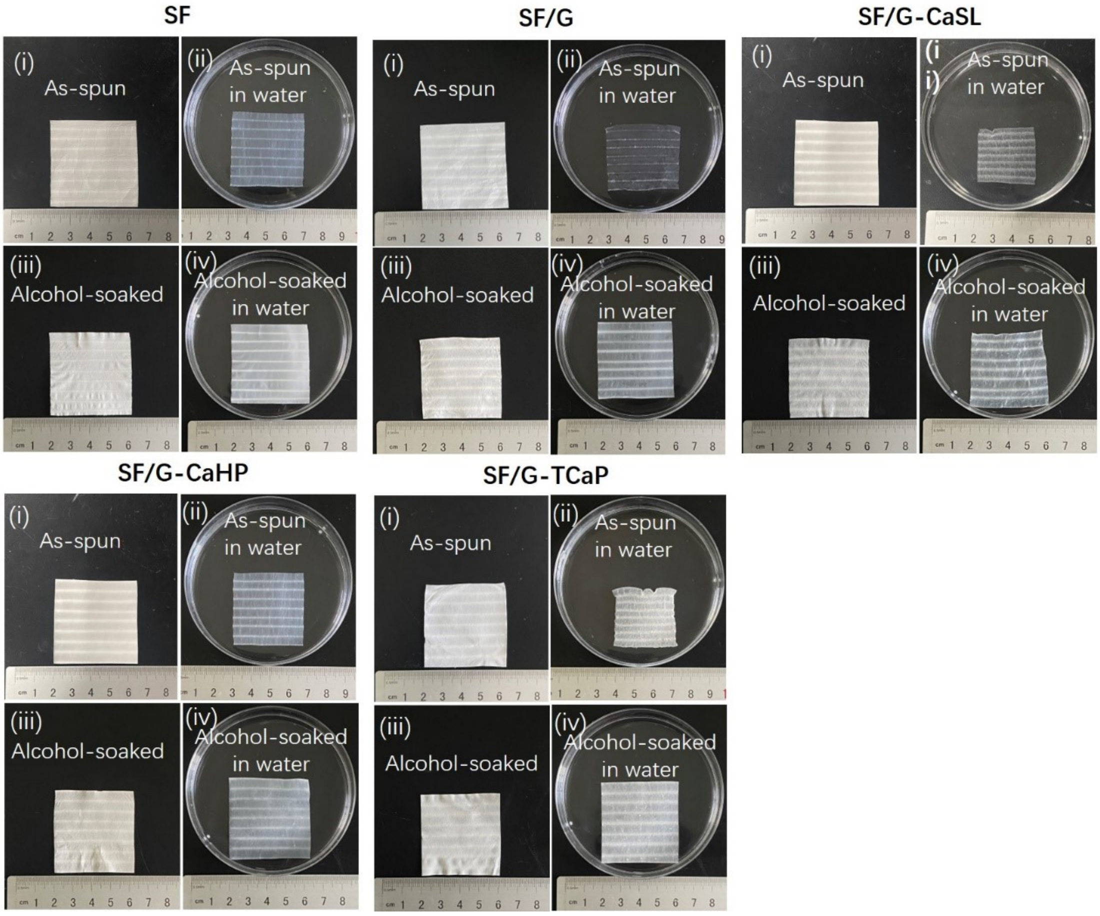

Figure S2. The as-electrospun ultrathin fibrous membranes were tailored into square (4.5 cm×4.5 cm) (i) and then soaked in water (ii) or treated by soaking in alcohol for 12 h and then dried at room temperature (iii). (iv) The alcohol-soaked fibrous membranes were further soaked into water.

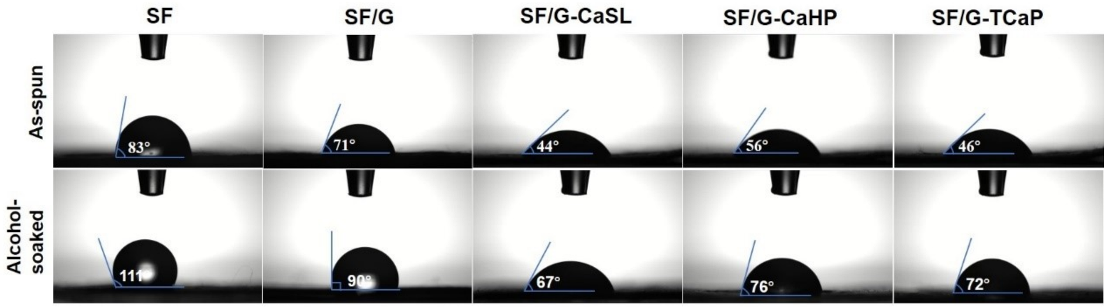

Figure S3. Water contact angle of the as-spun and alcohol-soaked fibrous membranes.

Table S3. The mechanical properties of the alcohol-soaked dry fibrous membranes.

	Tensile modulus [MPa]	Ultimate stress [MPa]	Elongation at break [%]
SF	257.14	4.3	4.71
SF/G	237.84	3.8	4.42
SF/G-CaSL	143.01	3.92	5.86
SF/G-CaHP	154.6	2.99	6.44
SF/G-TCaP	138.14	3.39	5.73

Table S4. The mechanical properties of the alcohol-soaked wet fibrous membranes.

	Tensile modulus [MPa]	Tensile strength [MPa]	Strain/Elongation at break [%]
SF	2.04	1.35	66.26
SF/G	1.65	0.78	47.43
SF/G-CaSL	2.12	0.57	47.29
SF/G-CaHP	0.96	0.44	45.84
SF/G-TCaP	1.3	0.52	39.9

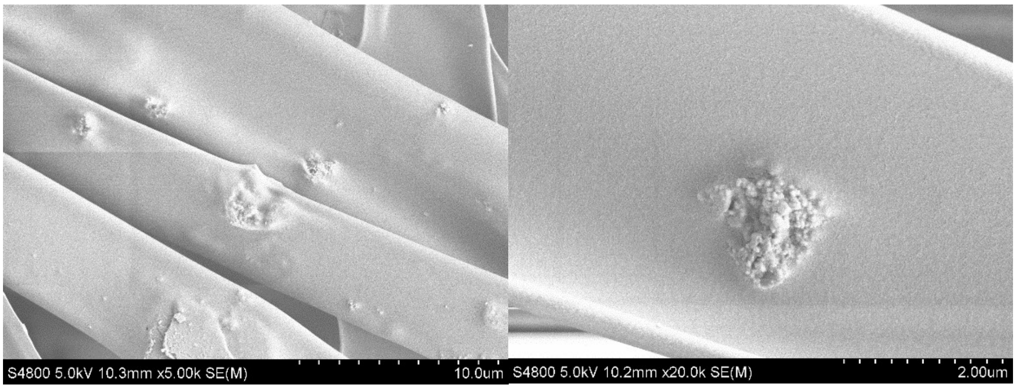

Figure S4. SEM image of the TCaP-loaded fibres, in which the TCaP aggregates were exposed on the fibrous surface.

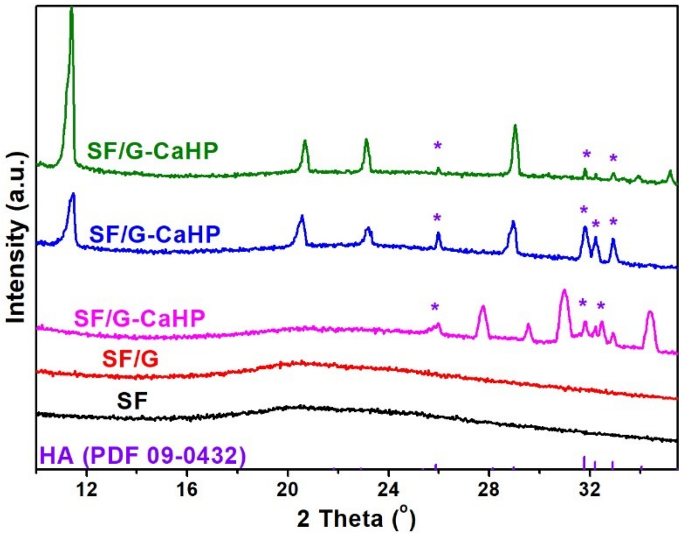

Figure S5. XRD patterns of the SBF-soaked fibrous membranes. The results showed that the HAP minerals formed in the CC-loaded fibrous membranes, but no HAP minerals deposited on the SF and SF/G fibrous fibers.